Comparative Study in the Structural and Modal Analysis of a Wind Turbine Planetary Gear Based on Material Reduction Criteria Using FEM

Abdellah Mohsine*, Boudi El Mostapha, Rabie El Alaoui, Kaoutar Daoudi
EMISys Research Team, Engineering 3S Research Center, Mohammadia School of Engineers, University Mohammed V in Rabat, Morocco.
Abdellah Mohsine: +212 606 103 638
‡*For correspondence: Email:* mohsine.abdellah@gmail.com

Received: 19.03.2019 Accepted: 06.05.2019

Abstract- With the increasing demand for energy from the effective and smart materials, the need to minimize vibration impacts in the most engineered parts of the machine is becoming a more important factor. Removing Vibrations are fundamental to their performance. In this study, results of a numerical simulation on the influence of material cutting of the planet gear on vibration of a wind turbine planetary gear are presented using Finite element Method. The aim of this paper is to create through cuts on the face profile of the planet gear body with different size (four different angle values α and four different radius values R) and to apply ANSYS software to determine and to compare the dynamical behaviors and also the natural vibration modes and forced harmonic frequency responses for the planetary gear with different planet gear cut size in order to validate the best construction of the 16 studied cases. The obtained result has shown that for the geometry with the material cutting parameter α =75°, R=16mm, the highest occurring stress is 43467 MPa for the frequencies between 4980 Hz and 5050 Hz. This stress value indicates the maximum value of the safety factor for the selected structure. So this chosen geometry represents the optimized design that makes it possible to economize the material and to reduce approximately 8.4% of the weight of the entire planetary gear of the wind turbine and so the vibrations of the entire planetary gear of the wind turbine could be reduced.

Keyword : vibration, material cut, frequency, planetary gear, harmonic response, Ansys

1. Introduction

Gearboxes are used in several types of industrial machines to provide the appropriate torque while reducing or multiplying the speed of rotation from a rotating power source using transmission gear ratios[1]. Gears are used in a variety of applications, such as wind turbines in our case, conveyors, draglines, cranes, new generation aircraft engines and many other machines. Gears are also used in automotive differential drives, final drives of heavy machinery, mainly as reducers[2], [3].

The performance of gear trains is influenced by many factors such the type and profile of the tooth, contact stresses, bearing number and type. These factors have been investigated with recent research approaches in [4]–[7].

Planetary gears can be used in wind turbines for many decades due to their compact design and high degree of efficiency[8]. Most of the wind turbines use a horizontal axis construction[9].

Since the wind turbine planetary gear includes components that directly convert the kinetic energy of the gear's rotation into electrical energy, it is essential to ensure the reliability of transmission designs to avoid shutdowns of the wind turbine. Due to the constant increase in wind turbine size, forces and emissions imply the influence of gearbox flexibility in the overall dynamic response of the Wind turbine [10], [11], which often leads to failure of gearbox components, particularly gears [12]–[15].

The failure of planetary gear components is currently one of the most problematic failures during the operational life-Cycle of a wind turbine. In particular, gearbox-related failures are responsible for more than 20% of wind turbine downtime failures. Generally, the expected lifetime results of the gearboxes are stated to be 20 years, but in practice, drive gearboxes must generally be replaced every 6 to 8 years [16], [17].

Many researchers have studied the static and modal analysis of planetary gears and the relationships between natural frequencies and the system parameters. Cunliffe et al. (1974) concentrated on an analytical planetary gear model with a fixed carrier and a characterized vibration mode [18]. Botman (1976) studied the impact of the planet gear axis loads on eigen natural frequencies using eighteen degres of freedom [19]. August and Kasuba (1986) used a torsional model with nine degrees of freedom to calculate torsional vibrations and dynamic loads in a standard planetary gear box system [20]. Kahraman (1993) and Sondkar and Kahraman (2013) studied three-dimensional modal deflection of a single and double helical planetary gear [21]. Tanna and Lim (2004) studied the modal

frequencies of ring gears and idealized smooth rings and they quantified the frequency differences by applying simpler smooth ring solutions to illustrate the initial modal behavior of ring structures [22].

The planetary gear unit is a supporting structure that must have sufficient stiffness to avoid resonance. Many research papers have proved the results of the ANSYS modal analysis with experimental results confirming the accuracy of the software [23]. In the case of frequent local defects, tooth wear, tooth cracks, tooth fractures and insufficient lubrication of the teeth are the main causes of vibrations in the gearbox which cause a broken tooth to cause maximum vibrations [24], [25]. Kalyanmoy Deb et al [26] optimized a multiple speed gearbox using different types of variables and parameters. They proved the use of a multiple objective evolutive algorithm that is capable to address the optimization's problem. Tianpei Chen et al. [27] utilized a differential evolutive algorithm for optimizing a two stage planetary gear system using the software mathematica. They demonstrated that the optimal planetary gear design could achieve the minimum volume (weight) under load capacity conditions. Jelen Stefanovic et. para. [28] published an article on the possibilities of the planetary gear optimization. They provided the original model for the multi criteria optimization of the planetary gear.

This mathematical model of the planetary gear optimization is described by the variables, objective functions and conditions necessary for its proper functionality and its performance[29]. Anjali Gupta et al. [30] investigated the optimization of a spur gear based on a genetic algorithm. They treated the central distance as a target function and the model parameters like the number of teeth, the modulus, the pitch diameter are considered as the variable. The bending and surface stress limits are considered as constraints.
K Akhilaet. al. [31] designed and analyzed a 3 stage planetary gear system that is used for a flying machine. It is designed to meet the output specifications and designed using CATIA Software to check the interferences. Designed components are checked out using ANSYS Software to check their mechanical properties. H. Jerrar [32] considered in his work four steps of material machining on the gear. He was able to reduce gear mass by 16% without any impact on the frequencies. Also he observed that the frequencies remain practically constant after machining more than 23 % of material. K. Daoudi [33] proposed a progressive material machining sequence by the variation of the width and the depth parameters of the circular pocket manufactured in planet gear. He could reduce 9.5 % of the planetary gear mass without any impact on the concentration of the constraint, the elastic deformation, and the displacement.

In this paper, static, modal and harmonic response analysis performed for different material cut size of a planet gear using the FEM Software Ansys 15.0 to find out and to compare the stress distribution, deformation, displacement, the natural frequencies and the mode shapes of the 16 studied cases using structure, modal and harmonic response analysis in ANSYS 15.0 in order to chose the best case in terms of material economy, weight and cost reduction.

2. Geometry

2.1. Part design

Generally, a single-stage planetary gear system is composed of a sun gear, a ring gear, a number of planets and a carrier. One of the components carriers, ring and sun can be selected as an input or output element and the power transmission is carried out through the Multiple Path of the planet gear Mesh. In this work, the carrier was selected as the input component and the sun gear was selected as the output. The parameters of the planetary gear teeth used in the study are given in Table 1.

Table 1. Calculation of Gear Parameters

Specification	ISO-Symbol	Formulas	Satellite (P)	Sun (S)	Ring (C)
Module	m	Standard values	1.5	1.5	1.5
Pitch primitive	P	P= πm	4.71	4.71	4.71
Number of teeth	Z		40	20	100
Pitch diameter	D	D=mZ	60	30	150
Foot diameter	D_f	D_f=D-2.5 m; D_f=D+2.5 m (C)	56.25	26.25	153.75
Head diameter	D_a	D_a=D+2m ; D_a=D-2m (C)	63	33	147
Base diameter	D_b	$Dcos\alpha$	56.38	28.19	140.95
Tooth width	b	B=Km K=10	15	15	15
Tooth height	h	H= h_a+ h_f=2.25m	3.38	3.38	3.38
Tooth thickness	E	E= πm/2	2.34	2.34	2.34
Pressure angle	α		20°	20°	20°

Figure 1 shows the planetary gear used in this work. The input in this particular planetary gear is the carrier, the output is the sun gear and the ring is fixed.

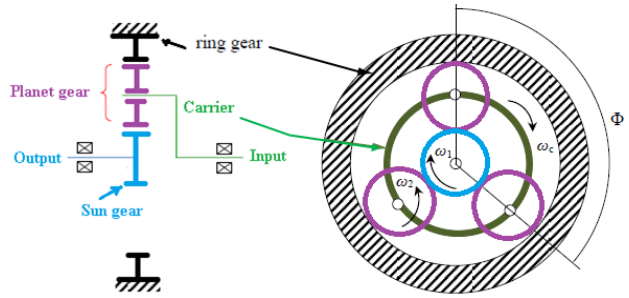

Fig. 1. The planetary gear used in this work.

2.2. The involute circle

The gears used in this work are spur gears and their tooth form has the shape of an involute curve driven by the parametrical equations. Those equations are written in Pro/ENGINEER Wildfire 4.0 using the following relation [34]:

$$Base\_circle\_radius = 28.2/2$$
$$Angle = t * 90$$
$$Cir\_len = (PI * Base\_circle\_radius * t)/2$$
$$X\_INS = Base\_circle\_radius * cos(Angle)$$
$$Y\_INS = Base\_circle\_radius * sin(Angle)$$
$$X = X\_INS + (Cir\_len * sin(Angle))$$
$$Y = Y\_INS - (Cir\_len * cos(Angle))$$
$$Z = 0$$

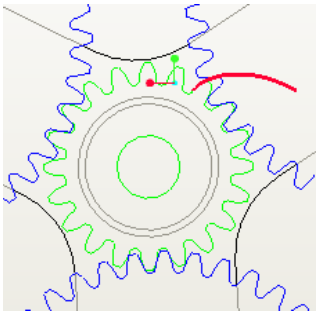

Fig .2. Involute curve of the teeth profile

2.3. Methodology

In this work we have considered two parameters for the through matrial cut of the planet gear: An angle α and a radius R. We have four angle (α=30°, α=45°, α=60° and α=75°) and for each angle there are four different radius (R=20mm, R=18mm, R=16mm and R=14 mm). It means that each through material cut is defined by an angle α and a radius R that starts from the reference line as shown in figure 3 a total number of 16 cases are to be analyzed. The first through material cut is defined by an angle of 30° and a radius of R=20 mm. The second one is defined by an angle of 30° and a radius of R=18mm. And so on. When the four conditions are done for the angle 30° we go to the second through material cut defined by an angle 45° and a radius with the four different values (R=20mm, R=18mm, R=16mm and R=14mm). We do the same until the all 16 cases are done.

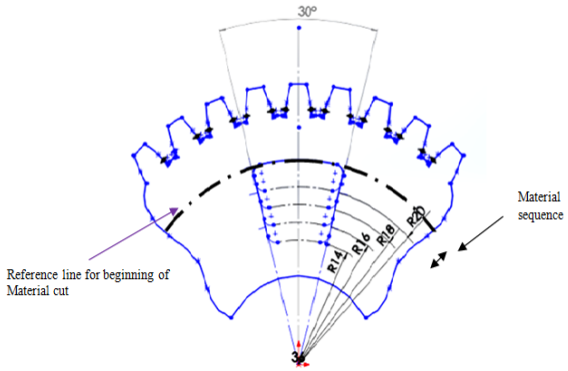

Fig. 3. Material cut parameters (angle α and Radius R)

The figure 4 shows the planet gear with the four through material cut defined by the four different angle.
When the geometry is done a static, modal and harmonic response analysis will be done using Simulation Software ANSYS 18.0.

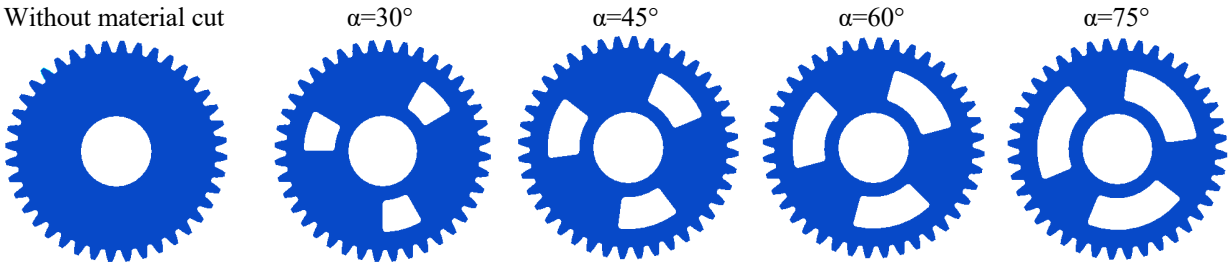

Fig. 4. Gear geometry evolution

After defining the involute circle, all the respective diameters have to be transferred and the successive operations of the basic schema in Figure 2 should be applied. Once this design process is completed, a through material cut with different size (with different angle and different radius) is created on the face of the planet gear and the finished model (Figure. 3)

is available to be exported as IGES file and imported into ANSYS 18.0 for the analysis. This model has been made simpler because it contains many symmetries and duplications. All gears (sun gear, planet gear and ring) are designed according to the same gear system parameters as presented in Table 1. The material properties of all gears are identical. Tempering, Hardening and other thermal processes of gears are not taken into account in this work. Only the gear material will be considered in the FEM analysis.

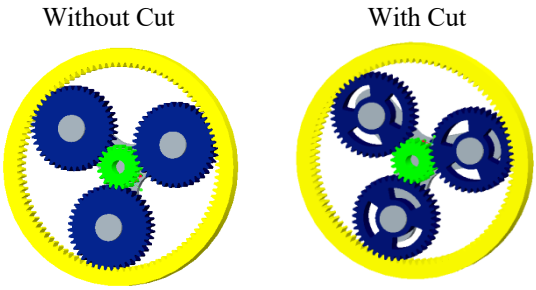

Fig. 5. Two representative geometries of the considered planetary gear

2.4. FEM Model

The FEM model is performed by ANSYS Workbench 15.0 Simulation software using the following steps:

- ✓ The 3D geometry of the different part geometries and their assembly were modeled with the Parametric Design Software Pro/ENGINEER Wildfire 4.0 M220;
- ✓ The planetary gear assembly were exported from Pro/ENGINEER Wildfire 4.0 in IGES format and imported in ANSYS Workbench Program (ANSYS 18.0);
- ✓ Choosing the proper analysis type: Static structural analysis.
- ✓ Definition of FEM static boundary conditions: The ring is fixed.
- ✓ Defining of material properties; here all gear and carrier materials are standard steel: Only Modulus of elasticity, Poison's Ratio and Density are required.
- ✓ Assignment of the loads for the static simulation: The moment is applied on the carrier shaft.
- ✓ Defining the contact type to determine how the contact surfaces can move relatively to one another. The choice of the appropriate type of contact depends on which type of problem you are trying to deal with. If the constraints are very close to a contact interface are significant, the non-linear contact types can be used. However, the choice of non-linear contact types will often provide a longer solution time and can regenerate convergence problems. In this study, friction and frictionless contact types are employed.
- ✓ Generation of the Mesh;
- ✓ Running the study;
- ✓ Analysis of the results.

2.5. Mesh

This is one of the main activities to convert the designed geometry into nodes and elements. This requires the geometry domain to be discretized into valuable areas for the analysis. After defining the model of the planetary gear in the FEM mode, we can generate a finite element mesh for it. Figure 6 shows the mesh geometry.

The contact of a single pair of teeth between the gears has been carefully aligned using PTC Software Pro/ENGINEER Wildfire 4.0. The tetrahedral element has been selected to create the FE mesh model of the planetary gear. The contact of a single pair of teeth between the gears has been carefully aligned using PTC Software Pro/ENGINEER Wildfire 4.0. The tetrahedral element was selected to create the FE mesh model of the planetary gear. The contact of the pair of teeth was aligned by touching each other tangentially. The contact surface between the gears has been set to be a rigid contact by selecting the "No separation" option, which is classified as a linear contact. With the finite element method, it is possible to solve many contact problems, from the basic to the most advanced, with a high degree of accuracy. The FEM can be considered the preferred method for dealing with contact problems because of its successful handling of mechanical issues in the field of solid mechanics, fluid mechanics, heat exchange [35]. This step is based on the composition of the model in finite elements. More the mesh size is small, more the accuracy is fine, more the resolution time is long. It is preferable to choose the automatic method in order to obtain standard results. Figure 6 shows the automatic planetary gear (with and without through material cut) meshing generated by Ansys 18.1 software.

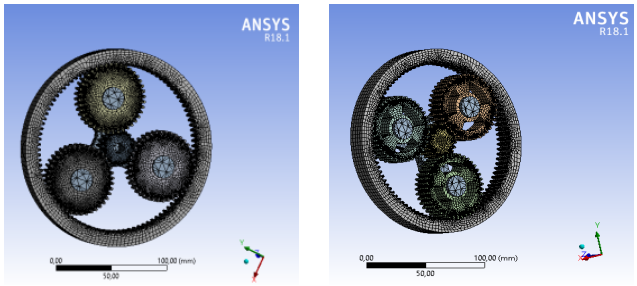

(a) (b)

Fig. 6. (a): FEM Model of Planet gear without material cut, (b): FEM Model of Planet gear with material cut (alpha=75° and R=14mm)

2.6. Boundary condition

The FEM Analysis and parameter studies were carried out in Ansys Workbench. Figure xxx shows the boundary conditions. The fixation is carried out on outside of the Ring. The Moment M=200 Nm is applied to the carrier shaft. The FEM Analysis is based on a linear elastic material model with an elasticity modulus of E=210000 N/mm².

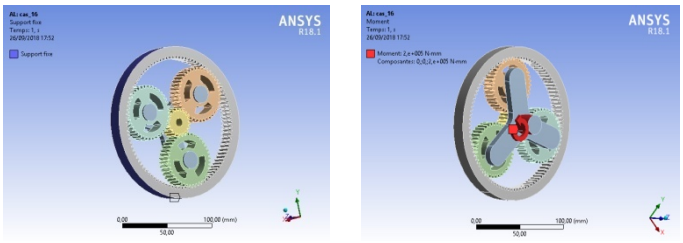

(a) (b)

Fig.7. (a): Support Ring fixed, (b): Moment on carrier shaft

3. Static Analysis simulation

The simulation is performed by ANSYS 18.1. The carrier is driven with a torque of 200Nm. The dimensions of the toothed wheels and the axis of the planet carrier as well as its speed of rotation are shown in Table 1 above. In this case the system is considered as static. In this document, the 3D geometry of the planetary gear system is modeled by the software Pro / ENGINNER Wildfire 4.0 and then transferred to Ansys 18.1 for a simulation. The statical and dynamical behaviors of the planetary gears are analyzed by the numerical method.

3.1. Results

The table below shows the different weight and volume values of the planetary gear in function of the different material cut on the planet gear.

Table 2. Weight and Volume of the Planetary Gear depending of the material cut parameters (angle and radius)

	Planet gear material cut (angle and radius)	**Weight of planetary gear [kg]**	**Volume of the planetary gear [mm³]**
Case_0	α=0° R=0mm	2,1904	2,7904e+005
Case_1	α=30° R=20mm	2,1556	2,7459e+005
Case_2	α=30° R=18mm	2,1377	2,7231e+005
Case_3	α=30° R=16mm	2,1198	2,7003e+005
Case_4	α=30° R=14mm	2,1019	2,6775e+005
Case_5	α=45° R=20mm	2,1345	2,7191e+005
Case_6	α=45° R=18mm	2,1060	2,6828e+005
Case_7	α=45° R=16mm	2,0776	2,6466e+005
Case_8	α=45° R=14mm	2,0492	2,6104e+005
Case_9	α=60° R=20mm	2,1156	2,6950e+005
Case_10	α=60° R=18mm	2,0777	2,6468e+005
Case_11	α=60° R=16mm	2,0399	2,5985e+005
Case_12	α=60° R=14mm	2,0020	2,5503e+005
Case_13	α=75° R=20mm	2,0989	2,6738e+005
Case_14	α=75° R=18mm	2,0528	2,615e+005
Case_15	α=75° R=16mm	2,0066	2,5561e+005
Case_16	α=75° R=14mm	1,9604	2,4973e+005

The Figure 8 shows that there is a significant reduction of the planetary gear weight. The weight value was equal to 2.1904 kg for the initial model of the planetary gear without material cut in the planet gear and it will be 1.9604 Kg for the model in the last machining sequence condition

(α=75°_R=14mm). It is a weight reduction of 10.5%. In the same way it is shown that a reduction of the volume of the planetary gear which can reach up to 8.9% for the model in the last machining sequence condition (α=75°_R=14mm) as shown in the figure 9.

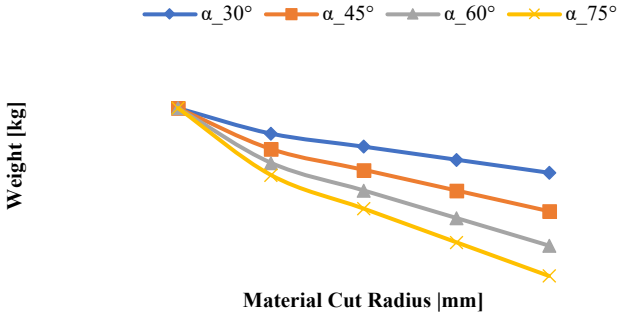

Fig. 8. The planetary gear weight in function of Material Cut

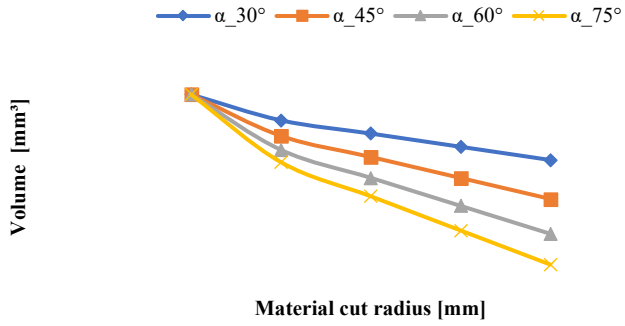

Fig. 9. The planetary gear volume in function of Material Cut

3.2. Static analysis

The next step in this numerical analysis is to obtain and to analyze the received results. The Ansys program provides a solution depending on the resolution type. Also FEM is used to perform the static analysis. This analysis of the planetary gear will be focused on the solutions regarding deformations, displacements and stresses of the planetary gear as shown in figure 10.

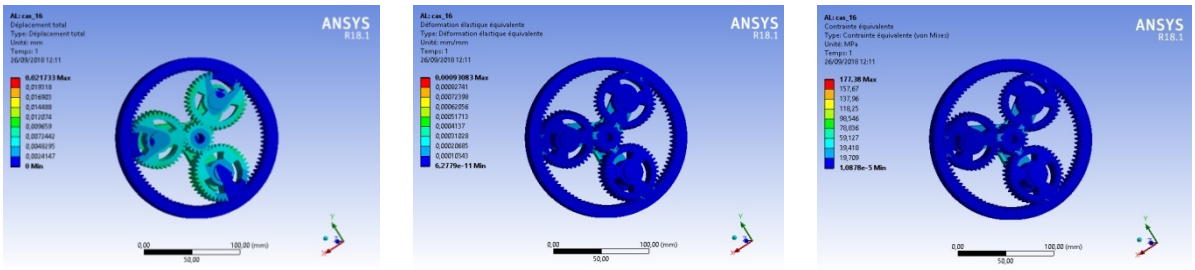

(a) Displacement (b) Deformation (c) Stress (Von Mises)

Fig. 10. Displacement, deformation and Stress Von Mises of the planetary gear

Figure 10: shows the graphical illustration of displacement, deformation and stress on the planetary gear for one of the 16 considered cases regarding the geometrical material cut conditions of the planet gear. A static analysis was first performed on the planetary gear where the planet gear doesn't contain any material cut. In this case, the maximum stress and maximum displacement occur on one side of the planet gear root fillet and are respectively 176.72 MPa and 2.11 e-2 mm (Figure 11). In the case where the material cut with different angle and radius dimensions is introduced into the planet gear, the maximum stress and maximum displacement occur at the same surface of the planet gear root fillet too and their values are in the same level as the geometry without material cut and don't exceeded respectively the values of 177.38 Mpa and 2.17 e-2 mm. This reflects a very small increase in stress (0.37%) and in displacement (2.6%) what can be accepted.

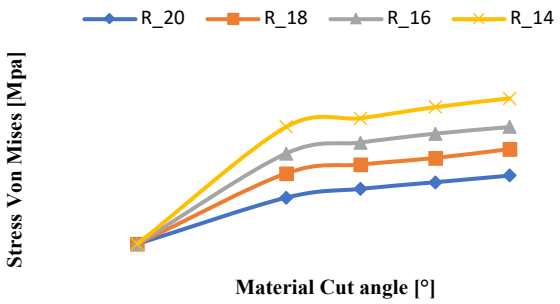

(a)

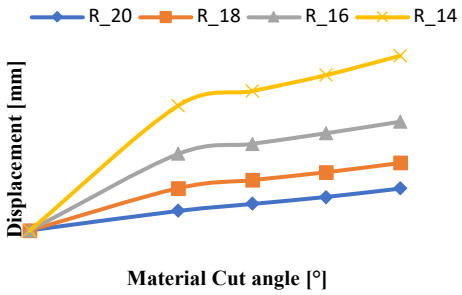

(b)

Fig 11. (a) Stress Von Mises in the planetary gear, (b) Displacement in the planetary gear for all cases

Comparisons have been performed with the finite element software Ansys 18.1 and applied to a planetary gear considering all 17 cases related to the material cut parameters in planet gear. The evolution of the stress and displacement for the all 17 cases is given in Figure 11 (a) and (b), it is observed that the results by the proposed approach compare well with the case where the planet gear geometry is without material cut which favours the use of the planet gear with a material cut which allows to save weight and material.

4. Modal analysis

Generally any physical model can generate vibrations. The frequencies and the modal shapes at which vibrations naturally appear are considered as model properties and can be analytically obtained by modal analysis. Modal analysis is a term used to describe the processes that are utilized to determine and to extract the modal properties of a model (Eigen frequencies, modal damping factors, and structural deformation called mode shapes) from structural information presented in a different format. Modal analysis helps to reduce the noise level of the product and to identify the causes of vibration generated by component cracking[36]. Also Modal analysis can improve the overall the product performance under certain operating conditions. In this paper the modal analysis performed on the software ANSYS 18.1 is considered as linear analysis. Any nonlinearity, such as plasticity, is ignored in this study. Natural frequencies and mode shapes are essential and significant parameters in the structure design for dynamic loading conditions. They are also necessary to perform a harmonic response analysis.
In terms of dynamic results, the proposed approach has been simulated for all 17 cases of the planet gear geometry without material cut and with material cut considering the different criterion (angle and radius).

As mentioned in the methodology above, 6 frequencies for all 17 considered cases (Material Cut on the planet gear with different angle and different radius) of the whole planetary gear will be determined and analyzed as shown in the figure 12.

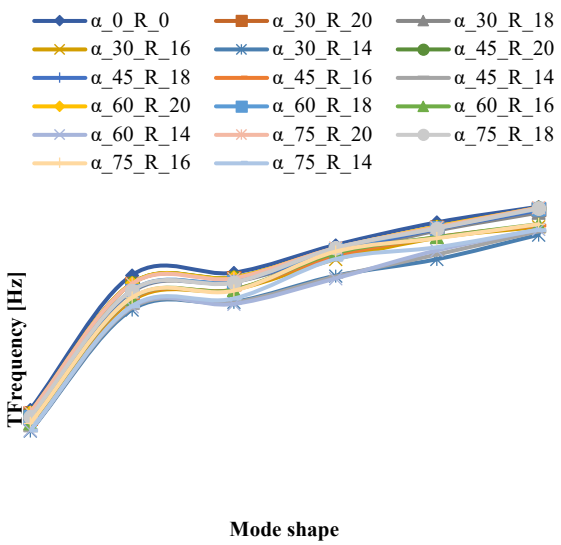

Fig. 12. First six natural frequencies of all considered cases of planetary gear geometry

According to the figure 12 it is to see that all frequencies have similar trajectories for all model geometries. It is to see too that the frequencies of the model without material cut are higher than the frequencies of all other models with different size of material cut. This is due to the relatively higher weight of the planet gear without material cut.

4.1. Convergence analysis:

In order to get trusted results, it is very necessary to verify that the solution is converged. As the planet gear undergoes different material cut, an adequate formulation must be consistent with the final solution of the model. In addition, a satisfactory convergence rate is also important in order to achieve acceptable accuracy. The convergence rate of a material cut operation can be obtained by study of results (frequencies) provided by a sequence of successively material cutting. The method consists of running the analysis on each planetary gear with defined material cut parameters on the planet gear (angle α and radius R). The results (frequencies) obtained from this analysis are compared with a second running analysis in which the material cut parameters (angle α and radius R) is different than in the previous analysis (Cook et al, 2002). The results of the two runs are compared with each other and so on and so forth until the percentage difference between solutions is equal or less than 2%.This percentage represents the descritization error. Accordingly this descritization error is calculated using the equation (1).

$$D_{ERROR} = \frac{X_{i+1} - X_i}{X_i} * 100 \quad (1)$$

where i represents the number of analysis and D_{ERROR} is descritization error. In this paper X refers to the determined frequency of the planetary gear.

As you can see from table 1 above, we have considered 4 different angles (α=30°, α=45°, α=60° and α=75°) for the material cut of the planet gear. For each angle we have taken 4 different radii which allow us to analyze a total of 17 cases considering the initial case without material cut (α=0° and R=0mm). Now, to make a selection of the better variant of geometry, we have established a criterion (descritization error) for all 4 cases, which helps us to validate the better geometry in terms of its result of modal analysis (frequencies) for each considered angle. At the end four better geometries are validated, which should also be compared with each other using harmonic response analysis and finally we get a better variant of the planet gear geometry, which can be selected for the design of the planetary gear.

- **CASE1 (α=30°).**

In the first case the angle of the material cut is fixed to α=30° and the radius is changed to the following values (R=20mm, R=18mm, R=16mm and R=14mm).

The table 3 below shows the six frequencies from the planetary gear of the initial case (planet gear without material cut α=0° and R=0mm) as well as the 6 frequencies from the planetary gear with different radius value of the material cut for the angle α=30°.

Table 3. Calculated frequencies for the planetary gear with the material cut parameter α=30°

	Frequency [Hz] α=0° R=0mm	Frequency [Hz] α=30° R=20mm	Frequency [Hz] α=30° R=18mm	Frequency [Hz] α=30° R=16mm	Frequency [Hz] α=30° R=14mm
1st	2427,5	2375	2326,8	2270	2228,5
2nd	4283,8	4167,9	4092,3	3991,2	3915,6
3rd	4318,1	4249,1	4186,8	4081,6	3992,2
4th	4700,9	4620,3	4571,1	4502,9	4409,3
5th	5013,5	4942,1	4900	4798,9	4694
6th	5229,8	5188,7	5148,3	5017	4910,6

In this dynamic simulation only 6 first frequencies are considered. And from the figure 13, we can make two main remarks: The first one is that all six calculated frequencies of the planetary gear increase with the shape mode in the 4 studied cases of geometry with material cut parameter α =30° and the initial geometry without removal of material independently of the material cut size on the planet gear. The second remark is that the difference between the 6 frequencies in each shape mode remains almost preserved und this difference does not exceed the value of 2.4% in the extreme case.

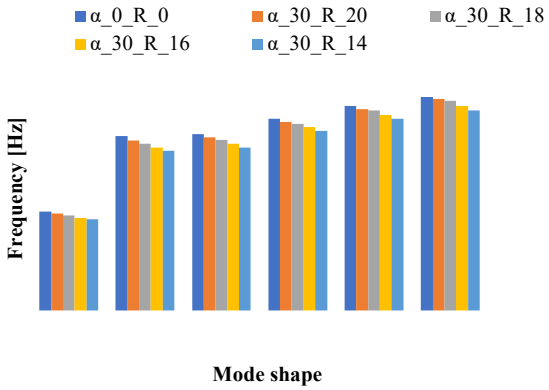

Fig. 13. Frequencies of the planetary gear with the material cut parameter α=30°

The results obtained are the subject of the descritization error calculation D_{ERROR} and from these results we draw the graph below (Figure 14) which is used to select and to validate the appropriate planet gear geometry of the four presented models.

DEROOR 1 represents the descritization error between the frequencies of the initial case without material cut and the frequencies of the followed geometry with the first material cut sequence α=30°, R=20mm. **DERROR 2** represents as well the descritization error between the planetary gear frequencies of the geometry with the second material cut sequence α=30°, R=18mm and the frequencies of the first material cut sequence α=30°, R=20mm. Also generally **DERROR i** represents the descritization error between the frequencies of the current geometry of material cut sequence and the frequencies of the geometry with the preceding material cut sequence.

Table 4. Descritization error calculation for the case α=30°

	D_{ERROR} 1	D_{ERROR} 2	D_{ERROR} 3	D_{ERROR} 4
1st	2,1627	2,0294	2,4411	1,8282
2nd	2,7055	1,8138	2,4705	1,8942
3rd	1,5979	1,4661	2,5127	2,1903
4th	1,7145	1,0648	1,4919	2,0787
5th	1,4241	0,8518	2,0632	2,1859
6th	0,7858	0,7786	2,5503	2,1208

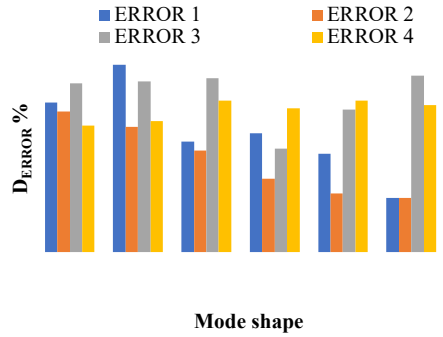

Fig. 14. Descritization error for the case α=30°

Also from the figure 14 it is to see that the planet gear with the geometry parameters (α=30°, R=14mm) is the appropriate variant as its solution is better converged since the percentage of descritization error D_{ERROR} is nearly to the fixed value of 2% (TABLE 4).

- **CASE2 (α=45°)**

In this case we set the material cut parameter α=45° and the radius R respectively to R=20mm, R=18mm, R=16mm and R=14mm which allows us to analyze five cases by considering the initial geometry without removing any material from the planet gear (α=0° and R=0mm).

The table 5 below shows the calculated 6 frequencies for the planetary gear considering the geometry condition of the planet gear with different material cut parameters as mentioned before.

Table 5. Calculated frequencies for the planetary gear with the material cut parameter α=45°

	Frequency [Hz] α=0° R=0mm	**Frequency [Hz] α=45° R=20mm**	**Frequency [Hz] α=45° R=18mm**	**Frequency [Hz] α=45° R=16mm**	**Frequency [Hz] α=45° R=14mm**
1st	2427,5	2382,3	2316,3	2259	2136,2
2nd	4283,8	4171,5	4065,2	3961,6	3830,5
3rd	4318,1	4253,8	4192,7	4085,1	3903,3
4th	4700,9	4640	4607,5	4552,5	4262,8
5th	5013,5	4952,9	4922,4	4809,3	4569,4
6th	5229,8	5206	5180,4	5045,3	4790,8

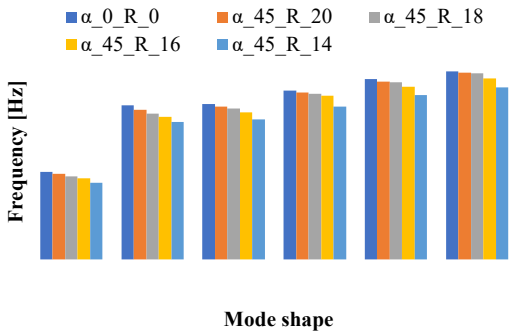

Fig. 15. Frequencies of the planetary gear with the material cut parameter α=45°

The figure 15 shows the graphical presentation of the calculated frequencies for the considered geometry. It is to see that the frequencies generally increase with the geometry material cut size and they have the same behavior as in the last case with the material cut parameter α=30°. It is to see that the first mode shape for all considered cases with alpha=45° refers to an average frequency value of 2300 Hz

where the last mode shape of all cases corresponds to an average frequency value of 4900 Hz.

Table 6. Descritization error calculation for the case α=45°

	D_{ERROR} 1	D_{ERROR} 2	D_{ERROR} 3	D_{ERROR} 4
1st	1,8620	2,7704	2,4738	5,4360
2nd	2,6215	2,5482	2,5485	3,3093
3rd	1,4891	1,4364	2,5664	4,4503
4th	1,2955	0,7004	1,1937	6,3635
5th	1,2087	0,6158	2,2977	4,9882
6th	0,4551	0,4917	2,6079	5,0443

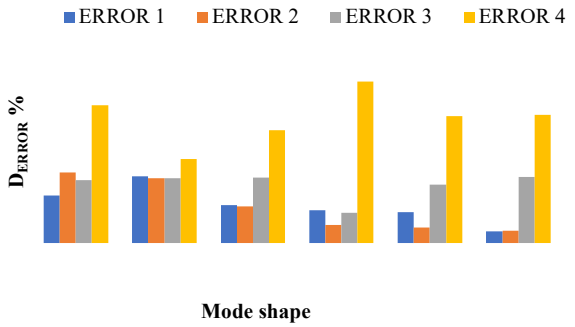

Fig. 16. Descritization error for the case α=45°

From the figure 16 it is to see that the planet gear with the geometry parameters (α=45°, R=16mm) is the appropriate variant as its solution is better converged since the percentage of descritization error D_{ERROR} is nearly to the fixed value of ca 2% (TABLE 5).

- **CASE3 (α=60°).**

with the same analogy as the processing of the last cases we set in this case the material cut parameter to α=45° and the radius R respectively to R=20mm, R=18mm, R=16mm and R=14mm which allows us to analyze five cases taking into account the initial geometry without removal of material from the planet gear (α=0° and R=0mm).

The table 7 below shows the calculated 6 frequencies for the entire planetary gear considering the geometry condition of the planet gear with different material cut parameters as mentioned before.

Table 7. Calculated frequencies for the planetary gear with the material cut parameter α=60°

	Frequency [Hz] α=0° R=0mm	Frequency [Hz] α=60° R=20mm	Frequency [Hz] α=60° R=18mm	Frequency [Hz] α=60° R=16mm	Frequency [Hz] α=60° R=14mm
1st	2427,5	2387,7	2322,9	2265,3	2138,8
2nd	4283,8	4171	4072,5	3966,4	3848,4
3rd	4318,1	4251	4191,6	4081,8	3885,4
4th	4700,9	4654,3	4639,2	4588,8	4238,3
5th	5013,5	4956,2	4934,5	4808	4627
6th	5229,8	5214,9	5199,6	5088,7	4715,3

Figure 17 shows a similar behavior of the frequency values as in the previous cases (α=30°, α=45°). The frequencies increase with the number of mode shape independently of the material cut cut size on the planet gear. It can be ssen too that the difference between the 6 frequencies in each mode shape remains nearly the same and doesn't exceed 2.4% in some extreme cases.

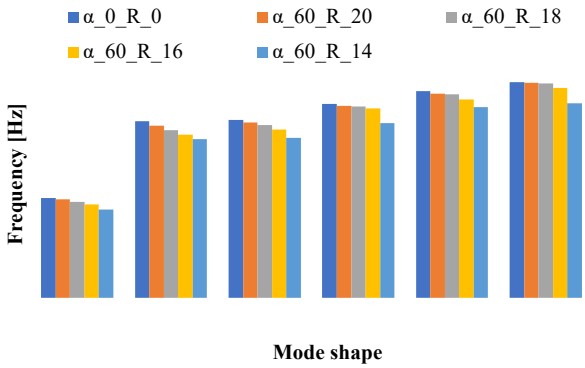

Fig. 17. Frequencies of the planetary gear with the material cut parameter α=60°

From the figure 18 it is to see that the planet gear with the geometry parameters (α=60°, R=16mm) is the appropriate variant as its solution is better converged since the percentage of descritization error D_{ERROR} is nearly to the fixed value of ca 2% (TABLE 8).

Table 8. Descritization error calculation for the caseα=60°

	D_{ERROR} 1	D_{ERROR} 2	D_{ERROR} 3	D_{ERROR} 4
1st	1,6395	2,7139	2,4797	5,5842
2nd	2,6332	2,3615	2,6053	2,9750
3rd	1,5539	1,3973	2,6195	4,8116
4th	0,9913	0,3244	1,0864	7,6382
5th	1,1429	0,4378	2,5636	3,7646
6th	0,2849	0,2934	2,1329	7,3378

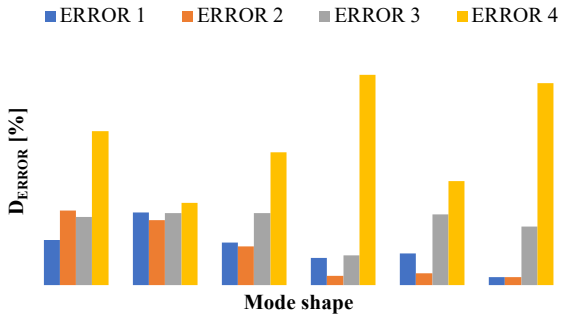

Fig. 18. Descritization error for the case α=60°

- **CASE4 (α=75°).**

With the same method as the previous cases, we set the material cut angle to α=75° and the radius R to the following values R=20mm, R=18mm, R=16mm and R=14mm respectively,. This will allows us to study five cases considering the initial geometry without removing material from the planetary gear (α=0° and R=0mm).

The table 9 below indicates the computed 6 frequencies for the entire planetary gear considering the geometry condition of the planetary gear with different material cutting parameters as mentioned above.

Table 9. Calculated frequencies for the planetary gear with the material cut parameter α=75°

	Frequency [Hz] α=0° R=0mm	Frequency [Hz] α=75° R=20mm	Frequency [Hz] α=75° R=18mm	Frequency [Hz] α=75° R=16mm	Frequency [Hz] α=75° R=14mm
1st	2427,5	2390	2326,1	2267,6	2197,6
2nd	4283,8	4164,5	4073	3973,4	3856,5
3rd	4318,1	4240,2	4181,4	4099,9	3960
4th	4700,9	4658,5	4657,9	4608,6	4504,5
5th	5013,5	4947	4930	4805,1	4669,8
6th	5229,8	5215,2	5205,9	5078,3	4912,1

The figure 19 shows the graphical presentation of the computed frequencies for the entire planetary gear. Similar to the cases we can see the increase of the frequencies with the mode shape. It can be observed that the first mode shape for all geometries studied in these cases with alpha=75° corresponds to an average frequency value of 2300 Hz, whereas the last mode shape of all cases refers to an average frequency value of 5070 Hz.

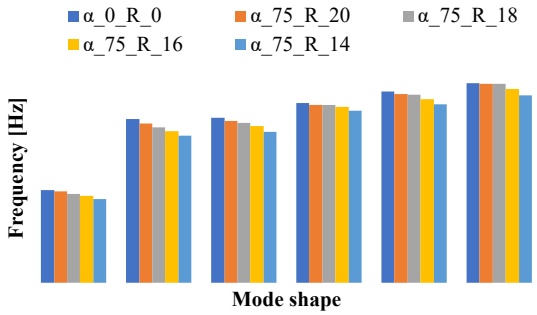

Fig. 19. Frequencies of the planetary gear with the material cut parameter α=75°

From the figure 20 it is to observe that the planet gear with the geometry parameters (α=75°, R=16mm) is the appropriate variant as its solution is better converged since the percentage of descritization error D_{ERROR} is nearly to the fixed value of ca 2% (TABLE 10).

Table 10. Descritization error calculation for the case α=75°

	D_{ERROR} 1	D_{ERROR} 2	D_{ERROR} 3	D_{ERROR} 4
1st	1,5448	2,6736	2,5149	3,0870
2nd	2,7849	2,1971	2,4454	2,9421
3rd	1,8040	1,3867	1,9491	3,4123
4th	0,9019	0,0129	1,0584	2,2588
5th	1,3264	0,3436	2,5334	2,8158
6th	0,2791	0,1783	2,4511	3,2727

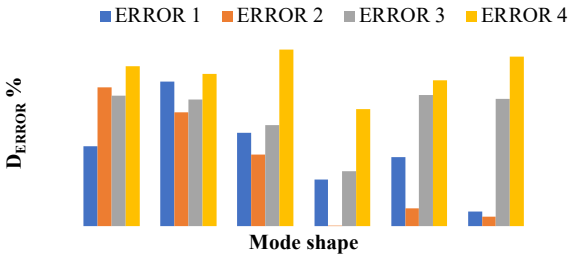

Fig. 20. Descritization error for the case α=75°

Based on modal analysis and descritization error D_{ERROR}, we were able to limit our choice on 4 planet gear geometries with the following parameters of material cutting (α_30_R_14, α_45_R_16, α_60_R_16 and α_75_R_16) as shown in the following Table 11.

Table 11. The appropriate geometry of the planet gear

	Frequency [Hz] α=30° R=14mm	Frequency [Hz] α=45° R=16mm	Frequency [Hz] α=60° R=16mm	Frequency [Hz] α=75° R=16mm
1st	2208,5	2259	2265,3	2267,6
2nd	3885,6	3961,6	3966,4	3973,4
3rd	3972,2	4085,1	4081,8	4099,9
4th	4395,3	4552,5	4588,8	4608,6
5th	4684	4809,3	4808	4805,1
6th	4891,6	5045,3	5088,7	5078,3

Those selected geometries in table 11 will be used for a harmonic response analysis in the following paragraph to make a convenient choice of an appropriate geometry of the planet gear.

5. Harmonic response analysis

Any persistent periodic load produces a persistent periodic response (a harmonic response) in a structural system. Harmonic Response Analysis is a method of predicting the persistent structure's dynamic behavior to determine whether or not the structure is successfully surmounting resonance, fatigue, and other adverse effects of induced vibration.

Harmonic response analysis needs periodic loading data for the analysis.

Now, in order to make a final selection of a geometry, we will perform a harmonic response analysis of the 4 selected geometries of Planet Gear. This analysis will allow us to predict the capacity of the structures to resist against dynamic effects. Also permits us to define the displacement and stress amplitude of the planetary gear caused by vibration for a given frequency which is already determined [37]. In this perspective, we have studied the four chosen cases according to the table 11.

In this harmonic analysis, the Young's Modulus, Poisson's Ratio, and Mass Density and the moment are required input where the moment is applied on the carrier shaft with the value of 200Nm and the condition that the ring is fixed.

The Stress and displacement amplitude of the different chosen models are illustrated in the following figures 21 and 22.

5.1. Stress

With the computational support of the harmonic response analysis using Ansys 18.0 the stress of the planetary gear over the whole frequency range from 2000 to 5500 Hz can be graphically represented. The peak values obtained in the frequency response diagrams were plotted. Figure 21 (a, b, c and d) shows the stress variations in the X, Y and Z directions with a specific frequency range. It is shown that for the case where the material cut is set to the parameters (α=30°and R=14mm) the maximum stress occurs on the root fillet of the gear in Y-axis and is 92440 MPa for the resonant frequencies between 4150 Hz und 4350 Hz, while at the case (α=45°, R=16mm) the maximum stress is 100600 MPa in X-axis for the resonant frequencies between 4750 Hz and 4900 Hz. When the material removal is done with the cut parameters (α=60° and R= 16mm) the maximal stress occurs in X-axis is 196200 MPa for the same frequency range as in the previous case (α=45°, R=16mm). For the case where the material cut is set to the parameters (α=75°, R=16mm) the maximal stress occurs in Y-axis and is 43467 MPa for the resonant frequencies between 4980 Hz and 5050 Hz.

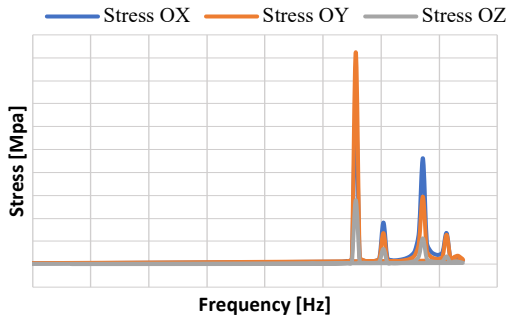

(a)

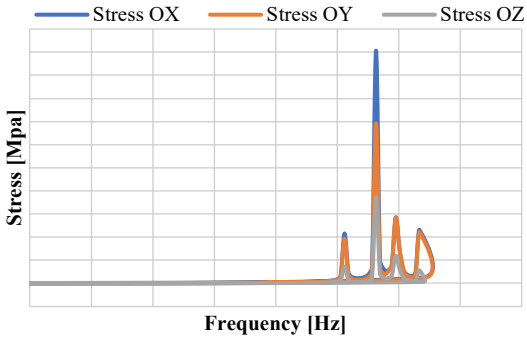

(b)

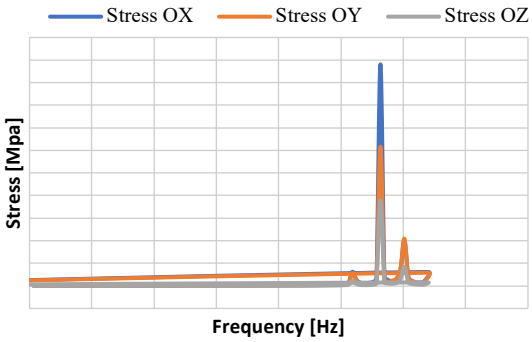

(c)

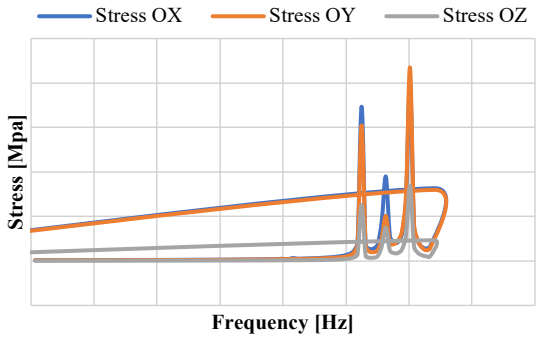

(d)

Fig. 21. Stress versus Frequency response
(a) : α=30°_R=14mm, (b): α=45°_R=16mm,
(c) : α=60°_ R=16mm, (d) : α=75°_ R=16mm

Table 12 below shows a summary of the maximum occurred stress in planetary gear in X, Y, Z directions for all considered cases of the material cut in the planet gear.

Table 12. Maximum stress for the four considered cases

Case α=30°, R=14mm	Max Stress (MPa)	Frequency [Hz]
X-Component	67585	4282
Y-Component	92440	4282
Z-Component	27917	4282

Case α=45°, R=16mm	Max Stress (MPa)	Frequency [Hz]
X-Component	1,006 e+005	4816
Y-Component	69226	4816
Z-Component	37449	4816

Case α=60°, R=16mm	Max Stress (MPa)	Frequency [Hz]
X-Component	1,962 e+005	4816
Y-Component	1,232 e+005	4816
Z-Component	75823	4816

Case α=75°, R=16mm	Max Stress (MPa)	Frequency [Hz]
X-Component	39907	5008
Y-Component	43467	5008
Z-Component	16865	5008

5.2. Displacement

The harmonic response analysis, as in the determination of stress amplitudes in the previous section, allows us to define the displacement amplitude of the planetary gear due to the vibration for a determined frequency ranges. So according to the limited four cases that we have chosen before in the table 11, the following vibration amplitude spectrums of the planetary gear displacements have been determined along the X, Y and Z directions as shown in figure 22.

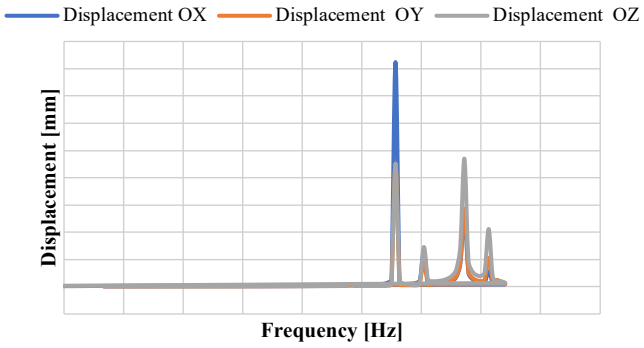

(a)

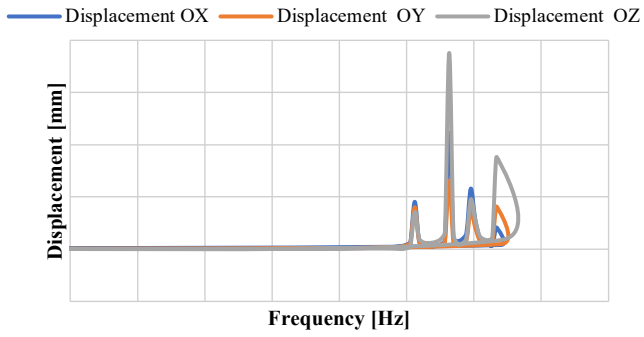

(b)

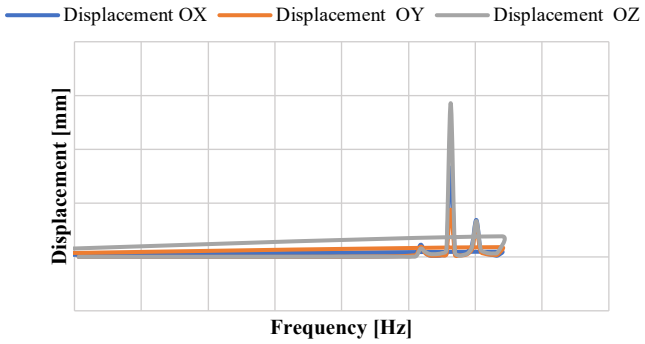

(c)

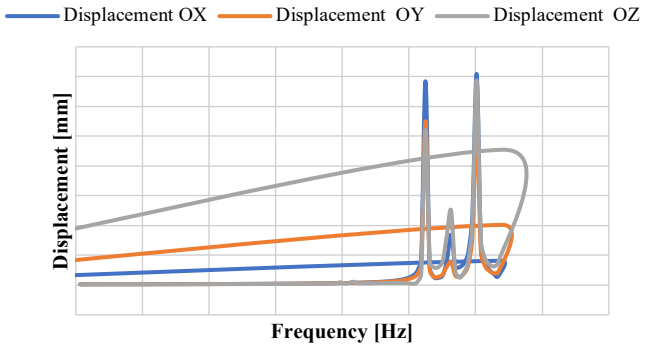

(d)

Fig.22. Displacement versus Frequency response
(a) : α=30°_R=14mm, (b): α=45°_R=16mm,
(c) : α=60°_R=16mm, (d) : α=75°_R=16mm

Similar to the previous section, the figure 22 shows the displacements of the planetary gear in x, y and z directions for the four cases. It can be shown that the maximal displacement occurs in X-axis and is 8.24 mm for the case where the material cut is set to the parameters (α=30°and R=14mm) for the resonant frequencies between 4150 Hz und 4350 Hz, while at the case (α=45°, R=16mm) the maximal displacement is 7.64 mm and occurs in Z-axis for the resonant frequencies between 4750 Hz and 4900 Hz. For the cases (c) and (d) the maximal displacements occur in Z-axis and are respectively 14.3 mm for the resonant frequencies that are between 4750 Hz and 4900 Hz and 3.5 mm for the resonant frequencies that are between 4980 Hz and 5050 Hz.

The table 13 below shows a summary of the maximum occurred displacement in planetary gear in X-, Y-, Z-directions for all considered four cases of the material cut in the planet gear.

Table 13. Maximum Displacement for the four chosen cases

Case α=30°, R=14mm	Max Displ. (mm)	Frequency [Hz]
X-Component	8,2424	4282
Y-Component	4,51	4282
Z-Component	4,7	4860

Case α=45°, R=16mm	Max Displ. (mm)	Frequency [Hz]
X-Component	4,46	4816
Y-Component	2,63	4816
Z-Component	7,515	4816

Case α=60°, R=16mm	Max Displ. (mm)	Frequency [Hz]
X-Component	8,31	4816
Y-Component	4,40	4816
Z-Component	14,3	4816

Case α=75°, R=16mm	Max Displ. (mm)	Frequency [Hz]
X-Component	3,541	5008
Y-Component	2,752	4624
Z-Component	3,4355	5008

6. Conclusion

A static analysis was first performed on the planetary gear, where the planet gear has no material cut. In this case, the maximum stress and maximum displacement occur on one side of the planet gear root fillet and are respectively 176.72 MPa and 2.11 e-2 mm. In the case where the material cut with different angle and radius dimensions is introduced into the planet gear, the maximum stress and maximum displacement occur at the same surface of the planet gear root fillet too and their values are in the same level as the geometry without material cut and don't exceeded respectively the values of 177.38 Mpa and 2.17 e-2 mm. This reflects a very small increase in stress (0.37%) and in displacement (2.6%). Also the performed simulation in the static analysis shows that the material cutting on the planet gear doesn't have any impact on the distribution of the stress, deformation and displacement which can validate the results obtained by K. Daoudi [33].

From the results of the harmonic response analysis basing on the modal analysis results it is to see that the maximum occurred stress obtained for all chosen cases is less than the maximum materials stress. Also the comparison of the appeared stresses and displacements in the planetary gear between the four chosen cases after the harmonic response analysis allows us to make the right choice of the geometry. So, for the geometry with the material cut parameter α =75°, R=16mm, the maximal occurred stress is 43467 MPa for the resonant frequencies between 4980 Hz and 5050 Hz. This value of stress gives maximum value of safety factor for the selected structure. So this selected geometry presents the optimized design that allows reducing the material and about 8.4% of the weight of the planetary gear which matches well with the tests performed by K. Daoudi [33]and consequently it allows the reduction of vibrations of the entire planetary gear of the wind turbine.

References

[1] A. Saxenaa, M. Choukseyb, A. Pareya 'Effect of mesh stiffness of healthy and cracked gear tooth on modal and frequency response characteristics of geared rotor system', *Mechanism and Machine Theory*, vol 107, pp. 261-273. Jan. 2017.

[2] G. Huang, S. Xu, W. Zhang, and C. Yang, 'Super-harmonic resonance of gear transmission system under stick-slip vibration in high-speed train', *Journal of Central South University*, vol. 24, no. 3, pp. 726–735, Mar. 2017.

[3] R. G. Parker, V. Agashe, and S. M. Vijayakar, 'Dynamic Response of a Planetary Gear System Using a Finite Element/Contact Mechanics Model', *Journal of Mechanical Design*, vol. 122, no. 3, p. 304, 2000.

[4] C. Fetvaci, 'Definition of Involute Spur Gear Profiles Generated by Gear-Type Shaper Cutters', *Mechanics Based Design of Structures and Machines*, vol. 38, no. 4, pp. 481–492, Oct. 2010.

[5] D. V. Muni and G. Muthuveerappan, 'A Comprehensive Study on the Asymmetric Internal Spur Gear Drives through Direct and Conventional Gear Design', *Mechanics Based Design of Structures and Machines*, vol. 37, no. 4, pp. 431–461, Oct. 2009.

[6] R. Thirumurugan and G. Muthuveerappan, 'Critical Loading Points for Maximum Fillet and Contact Stresses in Normal and High Contact Ratio Spur Gears Based on Load Sharing Ratio', *Mechanics Based Design of Structures and Machines*, vol. 39, no. 1, pp. 118–141, Jan. 2011.

[7] D. Icaza, S. Pulla, I. Colak, C. Flores, and F. Cordova, 'Modeling, Simulation and Stability Analysis of a Low-Wind Turbine for the Supply of Energy to the Amazon Jungle and Galapagos in Ecuador', in *2018 7th International Conference on Renewable Energy Research and Applications (ICRERA)*, Paris, pp. 100–105, 2018.

[8] C. O. Izelu and I. S. Oghenevwaire, 'A review on developments in the design and analysis of wind turbine drive trains', *International Conference on Renewable Energy Research and Applications (ICRERA)*, Milwaukee, WI, USA, pp. 589–594, 2014.

[9] Y. Yasa and E. Mese, 'Design and analysis of generator and converters for outer rotor direct drive gearless small-scale wind turbines', *International Conference on Renewable Energy Research and Application (ICRERA)*, Milwaukee, WI, USA, pp. 689–694, 2014.

[10] J. Helsen, G. Heirman, D. Vandepitte, and W. Desmet, 'The influence of flexibility within multibody modeling of multi-megawatt wind turbine gearboxes', *Proceedings of the International Conference on Noise And Vibration Engineering ISMA (2008)*, vol. 4, pp. 2045–2071, 2008.

[11] J. R. Cho, K. Y. Jeong, M. H. Park, and N. G. Park, 'Dynamic Response Analysis of Wind Turbine Gearbox Using Simplified Local Tooth Stiffness of Internal Gear System', *Journal of Computational and Nonlinear Dynamics*, vol. 10, no. 4, p. 041001, Jul. 2015.

[12] L. Hong, J. S. Dhupia, and S. Sheng, 'An explanation of frequency features enabling detection of faults in equally spaced planetary gearbox', *Mechanism and Machine Theory*, vol. 73, pp. 169–183, Mar. 2014.

[13] L. Hong and J. S. Dhupia, 'A time domain approach to diagnose gearbox fault based on measured vibration signals', *Journal of Sound and Vibration*, vol. 333, no. 7, pp. 2164–2180, Mar. 2014.

[14] Liu Hong and J. S. Dhupia, 'A time-domain fault detection method based on an electrical machine stator current measurement for planetary gear-sets', in *2013 IEEE/ASME International Conference on Advanced Intelligent Mechatronics*, Wollongong, NSW, pp. 1631–1636. 2013.

[15] J. Zhang, L. Hong, and J. Singh Dhupia, 'Gear Fault Detection in Planetary Gearbox Using Stator Current Measurement of AC Motors', *The AmericaSociety of Mechanical Engineers*, Fort Lauderdale, Florida, USA, vol. 1, pp. 673–680, Oct. 2012.

[16] S. Faulstich, B. Hahn, and P. J. Tavner, 'Wind turbine downtime and its importance for offshore deployment', *Wind Energy*, vol. 14, no. 3, pp. 327–337, Apr. 2011.

[17] L. F. Villa, A. Reñones, J. R. Perán, and L. J. de Miguel, 'Statistical fault diagnosis based on vibration analysis for gear test-bench under non-stationary conditions of speed and load', *Mechanical Systems and Signal Processing*, vol. 29, pp. 436–446, May 2012.

[18] F. Cunliffe, J. D. Smith, and D. B. Welbourn, 'Dynamic Tooth Loads in Epicyclic Gears', *Journal of Engineering for Industry*, vol. 96, no. 2, p. 578, 1974.

[19] M. Botman, 'Epicyclic Gear Vibrations', *Journal of Engineering for Industry*, pp. 811-814, Aug. 1976.

[20] R. August and R. Kasuba, 'Torsional Vibrations and Dynamic Loads in a Basic Planetary Gear System', *Journal of Vibration Acoustics Stress and Reliability in Design*, vol. 108, no. 3, p. 348, 1986.

[21] A. Kahraman, 'Planetary Gear Train Dynamics', *Journal of Mechanical Design*, vol. 116, no. 3, p. 713, 1994.

[22] R. P. Tanna and T. C. Lim, 'Modal frequency deviations in estimating ring gear modes using smooth ring solutions', *Journal of Sound and Vibration*, vol. 269, no. 3–5, pp. 1099–1110, Jan. 2004.

[23] R. V. Nigade, T. A. Jadhav, and A. M. Bhide, 'Vibration Analysis of Gearbox Top Cover', *International Journal of Innovations in Engineering and Technology*, vol. 1, no. 4, p. 8, 2012.

[24] M. R. G. Ghulanavar and M. V. Kharade, 'Conditioning monitoring of gearbox using vibration and acoustic signals', *International Journal of Advanced Technology in Engineering and Science*, vol. 3, no. 1, pp. 265–273, 2015.

[25] Y. Li, K. Ding, G. He, and H. Lin, 'Vibration mechanisms of spur gear pair in healthy and fault states', *Mechanical Systems and Signal Processing*, vol. 81, pp. 183–201, Dec. 2016.

[26] K. Deb and S. Jain, 'Multi-Speed Gearbox Design Using Multi-Objective Evolutionary Algorithms', *Journal of Mechanical Design*, vol. 125, no. 3, p. 609, 2003.

[27] T. Chen, Z. Zhang, D. Chen, and Y. Li, 'The Optimization of Two-Stage Planetary Gear Train Based on Mathmatica', in *Pervasive Computing and the Networked World*, vol. 7719, Q. Zu, B. Hu, and A. Elçi, Eds. Berlin, Heidelberg: Springer Berlin Heidelberg, 2013, pp. 122–136.

[28] S. I. Dilawer, A. R. Junaidi, and D. S. N. Mehdi, 'Design, Load Analysis and Optimization of Compound Epicyclic Gear Trains', *American Journal of Engineering Research*, p. 8, 2013.

[29] H. Nak and A. F. Ergenc, 'A new controller for variable speed wind turbine generator', *International Conference on Renewable Energy Research and Applications (ICRERA)*, Madrid, Spain, pp. 446–451, 2013.

[30] A. Gupta, 'Design Optimization of the Spur Gear Set', *International Journal of Engineering Research*, vol. 3, no. 9, p. 4, 2014.

[31] K. Akhila and M. A. Reddy, 'Design, modelling and analysis of a 3 stage epicyclic planetary reduction gear unit of a flight vehicle', *International Journal of Mechanical Engineering and Robotics Research*, vol. 3, no. 4, p. 9, 2014.

[32] H. Jerrar, A. E. Marjani, and M. Boudi, 'Use of Dynamic Behavior Criteria for Gear Shape Optimization', *Australian Journal of Basic and Applied Sciences*, p. 8, 2014.

[33] K. Daoudi and E. M. Boudi, 'Shape optimization of a planetary gear train based on the minimum weight', in *2016 International Renewable and Sustainable Energy Conference (IRSEC)*, Marrakech, 2016, pp. 1021–1024.

[34] A. Mohsine, B. E. Mostapha, and A. E. Marjani, 'Investigation of Structural and Modal Analysis of a Wind Turbine Planetary Gear Using Finite Element Method', *International Journal of Renewable Energy Research-IJRER*, vol. 2, pp. 753–760, 2018.

[35] 'Stresses and deformations in involute spur gears by finite element method.pdf', University of Saskatchewan Saskatoon, Saskatchewan, 2004.

[36] A. Harrouz, I. Colak, and K. Kayisli, 'Control of a small wind turbine system application', *International Conference on Renewable Energy Research and Applications (ICRERA)*, Birmingham, United Kingdom, pp. 1128–1133, 2016.

[37] Z. Zeng, J. Li, S. Zhang, Y. Hong, and Y. Wang, 'Analysis of the Harmonic Response of a Modulation Permanent Magnetic Transmission Equipment Based on ANSYS', *Energy and Power Engineering*, vol. 07, no. 03, pp. 63–70, 2015.